RAPID COMMUNICATIONS

PHYSICAL REVIEW B VOLUME 52, NUMBER 12 15 SEPTEMBER 1995-II

Spin-orbit coupling, exchange interaction, and hybridization in the photoexcitation of the Ni 3*p* core level

Y. Liu, Z. Xu,* and P. D. Johnson
Physics Department, Brookhaven National Laboratory, Upton, New York 11973

G. van der Laan
Daresbury Laboratory, Warrington WA4 4AD, United Kingdom
(Received 10 July 1995)

A spin-polarized photoemission study of the Ni 3*p* core level reveals the spin polarization of the main line and the satellites. A detailed comparison with calculation confirms earlier assignments that the satellites have d^9 character. However, the measurement also reveals the role of spin-orbit and exchange interactions in determining the spin polarization of the main peak, which is shown to be composed of both d^9 and d^{10} character. The study shows that the spin polarization in the leading edge of the main line reflects its d^9 character as a result of the hybridization between the different configurations.

Recently there have been several studies aimed at examining the possibility of using core-level spectroscopies as a probe of magnetic properties. The use of excitation from a core level is particularly appealing because it offers the possibility of studying site-specific information. The spectroscopies that have been investigated include spin-polarized core-level photoemission,[1–6] magnetic circular dichroism (MCD) in absorption[7,8] and photoemission,[9] and magnetic linear dichroism (MLD).[10,11] In the spin-polarized core-level photoemission experiment the spin of the photoemitted electron is measured directly; in the dichroism experiments the spin is coupled by the spin-orbit interaction. In all of these spectroscopies there are initial- and final-state effects, which include both the spin-orbit interaction and the exchange interaction. The coupling between the latter interactions will add complexity to the observed spectral density, particularly in the excitation of the 3*p* levels of the 3*d* transition metals, where they have similar magnitudes. An understanding of the coupling is therefore important if the different core-level spectroscopies are to be fully exploited.

In this paper we present the results of an experimental and theoretical study of the Ni 3*p* core-level photoemission where early experimental studies[12] indicate that the effect of the spin-orbit interaction is clearly observable. Our spin-polarized photoemission study provides important insight into the interplay between the spin-orbit coupling, exchange interaction, and hybridization or configuration interaction. Previous studies[12–14] have shown that excitation of both the valence band and core levels of Ni results in the appearance of main-line and satellite structure in the spectra. In particular, the 6-eV and 14-eV satellites observed during excitation of the 3*p* core level have been assigned to the $3p^53d^9$ configuration with the main line associated with a $3p^53d^{10}$ configuration. To our knowledge, there have been no detailed comparisons between experimental measurements of the spin polarization observed in the excitation and the theoretical predictions. In this paper, we present such a comparison. We are able to clearly show the role of the d^9 configuration in both the main line and the satellites. At the same time, we are able to make a detailed examination of the role of spin-orbit coupling and, further, the interplay between the latter and the exchange interaction. Not surprisingly, our analysis reverses some of the earlier theoretical assignments in the main peak. While the spin-orbit interaction produces the characteristic splitting in the d^{10} configuration, the strong hybridization with the d^9 configuration modifies the character of the main line. We find that the main peak's leading edge has predominantly $3p^53d^9$ character whereas a shoulder at higher binding energy reflecting the spin-orbit interaction has predominantly $3p^53d^{10}$ character. The spin-orbit interaction in the d^9 configuration, on the other hand, is largely quenched by the exchange interaction.

Our studies were carried out on the high-flux, high-resolution soft-x-ray X1B beamline at the National Synchrotron Light Source.[15] Spin-polarized photoemission is accomplished using a hemispherical analyzer backed by a low-energy spin detector[16] of the type developed by the National Institute of Standards and Technology group.[17] The latter detector is configured such that it can measure both longitudinal and transverse spin polarization in the emitted photoelectrons. The electron spectrometer collects electrons over a solid angle of $\pm 5°$. The incident photon energy used throughout the study was 248 eV. The overall energy resolution of the experiment was of the order of 0.6 eV.

The Ni film was produced by depositing Ni on a Cu(001) substrate to a thickness of the order of 25 ML. At such thicknesses, the Ni moments are found to align perpendicular to the surface, in agreement with earlier studies.[18] The data were collected in a geometry with the magnetization, the light polarization vector, and the electron acceptance in the same plane. In this way any added complexity due to chiral effects of the type described by Roth *et al.* are avoided.[10]

Figure 1 shows the spin-integrated and spin-resolved spectra obtained from the Ni 3*p* core level. The spin-integrated spectrum shows good agreement with the spectrum previously obtained by Hufner and Wertheim.[12] The main peak at a binding energy of approximately 66.8 eV shows the characteristic "spin-orbit splitting" *A*-*B* and satellites *C* and *D* occur at 6 and 14 eV higher binding energy. Figure 1 shows that the spin polarization is strongly concentrated in an intense feature at the leading edge of the main line. Whereas the polarization in the leading edge is strongly minority spin, the shoulder on the main peak shows a small majority-spin polarization. Satellite *C* shows minority- and

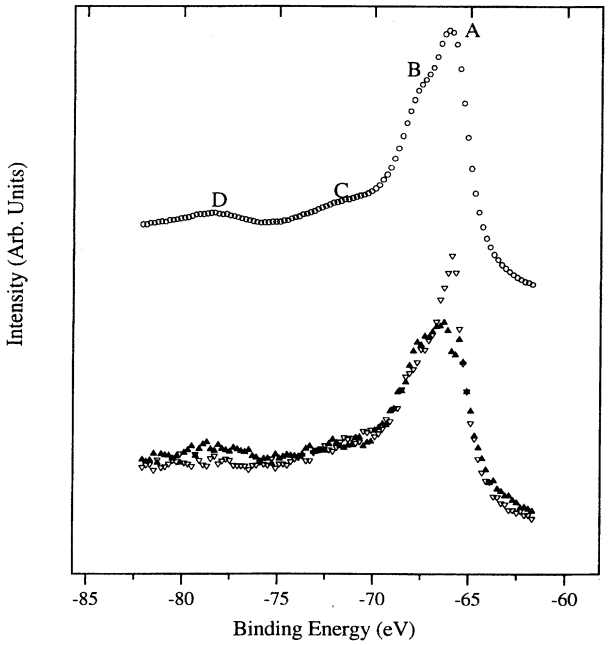

FIG. 1. Spin-integrated (upper spectrum) and spin-resolved (lower spectra) photoemission spectra of the Ni $3p$ core level. A-B indicate "spin-orbit"-derived features in the main line and C and D indicate satellite features. In the lower panel the minority-spin electrons are indicated by the open triangles and the majority-spin electrons are indicated by the filled triangles. The incident photon energy is 248 eV.

satellite D majority-spin polarization.

Since the satellite structure is of many-particle origin,[12] we have calculated the Ni $3p$ photoemission spectrum [Fig. 2(a)] with an Anderson impurity model including multiplet structure using the Cowan program.[19] Because of the small polarization and to facilitate comparison between theory and experiment, we show in Fig. 2(b) the theoretically determined difference between the majority- and minority-spin spectra. In Fig. 2(c) we show the same experimentally determined difference spectrum, I_0P, where I_0 is the spin-integrated intensity and P is the measured spin polarization. It is clear from the comparison in Fig. 2 that all of the features observed in the experimental spectra are reproduced in the calculation.

In the calculation a particular site in the Ni metal is treated with a basis set d^8, $d^9\underline{v}$, and $d^{10}\underline{v}^2$, where $\underline{v}$ denotes a combination of orbitals of appropriate symmetry on adjacent sites. For brevity we will drop the $\underline{v}$ in the notation. The energies of these basis states are 0, $\Delta-U$, and $2\Delta-U$, respectively, where $\Delta=E(d)-E(v)$ is the transfer energy and U is the d-d Coulomb interaction. For simplicity, we omit crystal field symmetry and use an isotropic mixing parameter V.[20] The final states are a mixture of the $\underline{c}3d^8$, $\underline{c}3d^9$, and $\underline{c}3d^{10}$ configurations with relative energies of 0, $\Delta-U-Q$, and $2\Delta-U-2Q$, respectively. Here $\underline{c}$ denotes the $3p$ core hole, and Q is the $3p$-$3d$ Coulomb interaction (the effective Slater parameter F^0). The molecular field (exchange field) acting on the $3d$ spins is included by a term $g\mu_BHS$, with $g\mu_BH=-0.5$ eV. These values result in a ground state of 14% d^8, 48% d^9, and 38% d^{10} character, which compares well with previous calculations.[21,22] The configurations with

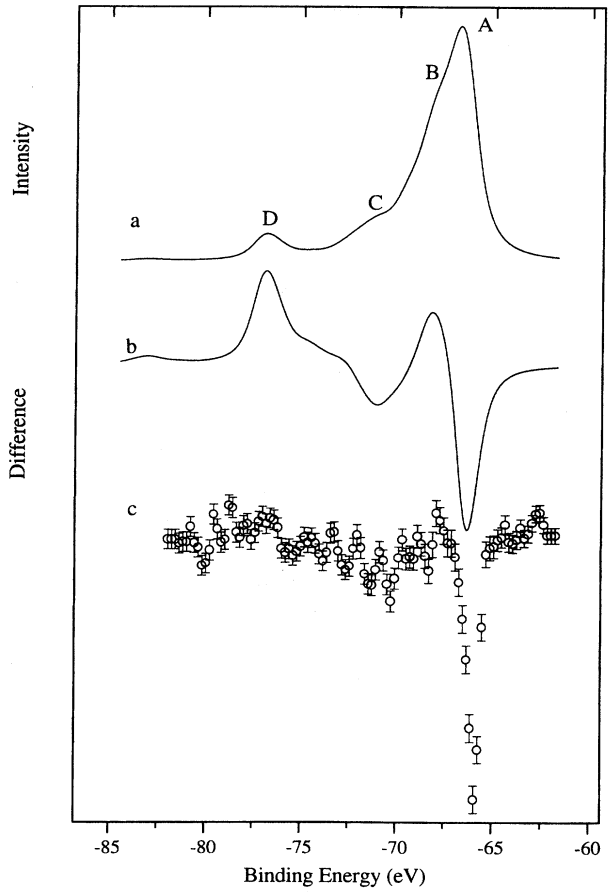

FIG. 2. (a) Calculated spin-integrated spectrum for the Ni $3p$ core level. (b) Calculated difference spectrum between the two spin components through the Ni $3p$ core-level region. (c) Experimentally determined difference between the two spin components in Fig. 1. A smoothing routine has been applied to the latter spectrum.

open shells show a term splitting due to the spin-orbit interactions $\zeta(3p)=1.37$ and $\zeta(3d)=0.09$ eV, and the Slater parameters $F^2(dd)=13.3$, $F^4(dd)=8.3$, $F^2(pd)=13.6$, $G^1(pd)=16.9$, and $G^3(pd)=10.3$ eV. To account for intra-atomic relaxation effects, these Hartree-Fock values of the Slater integrals were scaled to 65% and the $3p$ spin-orbit interaction to 85%. The calculated spectra were convoluted with a Lorentzian of $\Gamma=0.6$ eV and a Gaussian of $\sigma=0.4$ eV to account for the core-hole lifetime and the instrumental broadening. The best fit to the experiment was obtained with $\Delta=-0.75$, $U=1.5$, $Q=2$ eV, and $V=0.8$ eV.

One may interpret the photoemission spectrum in Fig. 1 as consisting of a main peak with $\underline{c}3d^{10}$ character, which is split by spin-orbit interaction, and a satellite structure with $\underline{c}3d^9$ character. However, such an assignment would not explain the fact that the leading edge of the main peak displays a very strong spin polarization. Since a $\underline{c}3d^{10}$ state cannot be spin polarized, the peak assignment must have more to it.

Figure 3 shows the decomposition of the photoemission spectrum into the contributions from the $\underline{c}3d^{10}$, $\underline{c}3d^9$, and $\underline{c}3d^8$ configurations and their interference terms. The origin of the interference terms in a simplified model is the following: given a ground state $\psi_i=\alpha d^{10}+\beta d^9$ and a final state

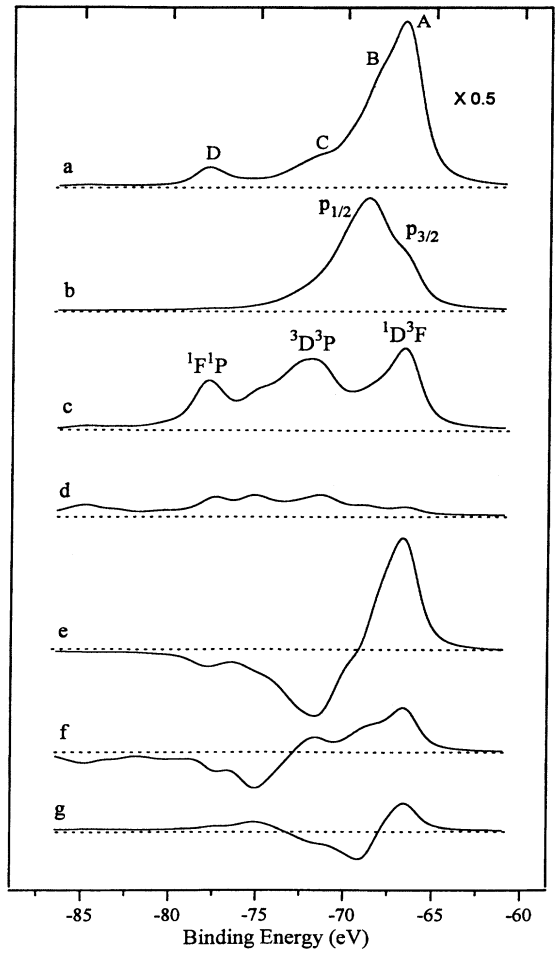

FIG. 3. The different contributions to the spin-integrated theoretical spectrum shown in (a) are (b) $\underline{c}3d^{10}$, (c) $\underline{c}3d^9$, and (d) $\underline{c}3d^8$. The interference terms between the different configurations are indicated by (e) $\underline{c}3d^{10}$ and $\underline{c}3d^9$, (f) $\underline{c}3d^9$ and $\underline{c}3d^8$, and (g) $\underline{c}3d^{10}$ and $\underline{c}3d^8$.

$\psi_f = \gamma \underline{c}d^{10} + \delta \underline{c}d^9$, the intensity of the $\underline{c}3d^{10}$ and $\underline{c}3d^9$ configurations and interference term is proportional to $(\alpha\gamma)^2$, $(\beta\delta)^2$, and $\pm 2\alpha\beta\gamma\delta$, respectively. The + and − signs represent a bonding and antibonding state, respectively. Although the situation in Fig. 3 is more complicated than such a 2×2 matrix model, the bonding and antibonding parts in the interference terms are clearly visible with positive and negative intensities, respectively, at low and high binding energies.

Figure 3(b) shows that the $\underline{c}3d^{10}$ configuration is split by the spin-orbit interaction into a $p_{3/2}$ and a $p_{1/2}$ level. However, the intensity ratio is not the statistical 2:1 ratio, because of the different mixing of these levels with the singlet and triplet states of the $\underline{c}3d^9$ configuration.

Figure 3(c) shows that the $\underline{c}3d^9$ configuration is split by the large $3p$-$3d$ electrostatic interaction into three clearly distinguishable features, which, in order of increasing binding energy, correspond to the ^3F and ^1D states, the ^3P and ^3D states, and the ^1P and ^1F states. Thus the ^3F state corresponds to the main peak's leading edge. The interference between the $\underline{c}3d^{10}$ and $\underline{c}3d^9$ channel transfers spectral weight from satellite C in the $\underline{c}3d^9$ spectrum to the main peak. It is this strong $\underline{c}3d^9$ character that is the reason for the strong spin polarization at the onset of the main peak. The singlet $\underline{c}3d^9$ states are completely spin-up polarized, while the triplet states have a spin-up to spin-down ratio of 1:2 resulting in a net spin-down polarization. From the spin spectrum [Fig. 2(b)] it is also clear that the singlet and triplet character of the individual satellites is largely retained and that the separation of the two satellites is a measure of the $3p$-$3d$ exchange interaction. The influence of the spin-orbit interaction in the $\underline{c}3d^9$ configuration is small because it is largely quenched by the electrostatic interactions. Finally, we comment that the $\underline{c}3d^8$ character becomes relatively important only at the high-binding-energy side of the spectrum.

The high-binding-energy shoulder of the main peak has mainly $\underline{c}3d^{10}$ character. The energy separation of this shoulder from the main peak is of the order of the $3p$ spin-orbit splitting. Indeed, in a spectrum calculated without the spin-orbit interaction the shoulder disappears. Thus the splitting in the main peak can indeed be ascribed to the spin-orbit interaction and not to an exchange splitting. However, by such an assignment, it is important to keep in mind that, due to the strong mixing, *the spin-orbit doublet partner at low binding energy has much more d^9 character and the partner at higher binding energy has more d^{10} character.* In a calculation with the spin-orbit interaction included but without the mixing the d^{10} spectrum shows the characteristic 2:1 intensity ratio of the spin-orbit split doublet.

The present study provides insights into the interplay between the spin-orbit interaction and the Coulomb interaction in the excitation of the Ni $3p$ core level. The spin-orbit interaction plays the most important role in the structure or spectral density associated with the $\underline{c}3d^{10}$ configuration. However, the strong hybridization with the $\underline{c}3d^9$ configuration considerably reduces the intensity of the lower-binding-energy component. In the $\underline{c}3d^8$ and $\underline{c}3d^9$ configurations the influence of the spin-orbit interaction is less because it is quenched by the Coulomb interactions. These observations have implications for recent theoretical analyses[23,24] of the spectra obtained in spin-polarized photoemission studies of the Fe $3p$ core level[1,2] and related MLD studies,[10] where the interplay of the spin-orbit and exchange interactions adds considerable complexity to the interpretation.

For Cu, Ni, Co, and Fe, the Hartree-Fock values of $\zeta(3p)$ are 1.62, 1.37, 1.15, and 0.95 eV, respectively.[25] In the absence of an exchange interaction the spin-orbit splitting will be 1.5ζ and indeed such a value has recently been found in MLD studies of the Cu $3p$ level.[26] However, it is remarkable that such a large splitting is not observed in the $3p$ photoemission spectra from systems with partly filled $3d$ shells. Tamura *et al.*,[24] in their modeling of the Fe $3p$ MLD spectra, found the best agreement using 60% of the spin-orbit parameter value from band-structure calculations. The spin-orbit splitting will be especially visible in spin-resolved photoemission since the $p_{3/2}$ level has dominantly minority spin and the $p_{1/2}$ has dominantly majority spin. The spin-difference spectrum will then show a negative and a positive structure with a separation of 1.5ζ. Also, the magnetic dichroism, which is sensitive to the orbital magnetization, will show a peak splitting due to the spin-orbit interaction which couples the orbit and the spin parallel and antiparallel at low and high binding energies, respectively.

The peak splitting will become even larger if we take into account an effective (one-electron) exchange interaction, which results in a further bifurcation of minority-spin character at low binding energy and majority-spin character at high binding energy. The increase in the splitting will be especially strong when the exchange interaction and the spin-orbit interaction are of the same order of magnitude. Therefore, while a single-particle model gives a correct result for the deeper core levels, such as the $2p$ level, it overestimates the peak splitting for shallow core levels where neither the spin-orbit nor exchange interaction can be treated as a perturbation.[27]

This problem can be overcome in a localized model, where the configurations $\underline{c}d^n$ with $n \neq 10$ have strong term splittings which may partly quench the spin-orbit interaction. Although this can result in a broad multiplet structure spread out over 10 or 20 eV, the hybridization will strongly reduce the high-binding-energy satellites in the spectrum. The amount of hybridization between the individual levels in the $\underline{c}d^n$ and $\underline{c}d^{n-1}$ configurations depends on their energy difference, which is not only determined by the charge-transfer Δ and the Coulomb interactions U and Q, but especially by the term splitting that is governed by the Slater parameters F and G.

Using the Ni $3p$ as an example, in the initial state the d^9 configuration is lower in energy than the d^{10} configuration. In the final state the average energy of the $\underline{c}d^{10}$ is lower than the average of the $\underline{c}d^9$ configuration. Thus, without term splitting, the low-binding-energy side would have $\underline{c}d^{10}$ character, and the $\underline{c}d^9$ satellite intensity would be large. However, the large term splitting, as evidenced by the separation between the structures C and D in the experimental spectrum, pushes the ^3F level below the $\underline{c}d^{10}$ level. This results in a strong interference term for the triplet states (Fig. 3). A maximum interference term would be obtained if the final-state wave function has coefficients $\gamma=\alpha$ and $\delta=\beta$, in which case the satellite intensity vanishes completely and all intensity goes into the main peak. Thus the reduction of the $3p$ spin-orbit interaction in Fe and Co might be due to the combined presence of a strong hybridization between many configurations and large term splittings. Unfortunately, the Anderson impurity calculations for Fe and Co are far from trivial. Although these model calculations inevitably contain optimized or estimated parameters, they provide a useful insight into the correlation effects which are present in $3d$ metals. Such an insight cannot be obtained from a single-particle model.

It is not expected that a general rule can be given on whether an observed $3p$ splitting in the $3d$ metals is either due to term splitting, hybridization, exchange interaction, or spin-orbit coupling. This is already apparent in our analysis of the Ni $3p$ spectrum, which shows that the peak structure is due to the interplay of all these effects. However, in the case of nickel one might say that the main peak splitting is due to the spin-orbit splitting which is surviving in the $\underline{c}d^{10}$ configuration. To solve the question for the other $3d$ metals requires both better spin-resolved or magnetic dichroism photoemission data and more elaborate many-particle calculations.

This work was supported in part by the Department of Energy under Contract No. DE-AC02-76CH00016.

*Present address: Advanced Photon Source, Argonne National Lab, Argonne, IL 60439.

[1] C. Carbone and E. Kisker, Solid State Commun. **65**, 1107 (1988).
[2] B. Sinkovic, P. D. Johnson, N. B. Brookes, A. Clarke, and N. V. Smith, Phys. Rev. Lett. **65**, 1647 (1990).
[3] F. U. Hillebrecht, R. Jungblut, and E. Kisker, Phys. Rev. Lett. **65**, 2450 (1990).
[4] C. Carbone, T. Kachel, R. Rochow, and W. Gudat, Solid State Commun. **77**, 619 (1991).
[5] F. U. Hillebrecht, Ch. Roth, R. Jungblut, E. Kisker, and A. Bringer, Europhys. Lett. **19**, 711 (1992).
[6] D. G. Van Campen, R. J. Pouliot, and L. E. Klebanoff, Phys. Rev. B **48**, 17 533 (1993).
[7] G. Schutz, W. Wagner, W. Wilhelm, P. Kienle, R. Zeller, R. Frahm, and G. Materlik, Phys. Rev. Lett. **58**, 737 (1987).
[8] C. T. Chen, F. Sette, Y. Ma, and S. Modesti, Phys. Rev. B **42**, 7262 (1990).
[9] L. Baumgarten, C. M. Schneider, H. Petersen, F. Schafers, and J. Kirschner, Phys. Rev. Lett. **65**, 492 (1990).
[10] Ch. Roth, F. U. Hillebrecht, H. B. Rose, and E. Kisker, Phys. Rev. Lett. **70**, 3479 (1993).
[11] F. Sirotti and G. Rossi, Phys. Rev. B **49**, 15 682 (1994).
[12] S. Hufner and G. K. Wertheim, Phys. Lett. **51A**, 301 (1975).
[13] W. Eberhardt and E. W. Plummer, Phys. Rev. B **21**, 3245 (1980).
[14] G. van der Laan, M. Surman, M. A. Hoyland, C. F. J. Flipse, B. T. Thole, Y. Seino, H. Ogasawara, and A. Kotani, Phys. Rev. B **46**, 9336 (1992).
[15] K. J. Randall, J. Feldhaus, W. Erlebach, A. M. Bradshaw, W. Eberhardt, Z. Xu, Y. Ma, and P. D. Johnson, Rev. Sci. Instrum. **63**, 1367 (1992).
[16] Zhongde Xu and P. D. Johnson (unpublished).
[17] J. Unguris, D. T. Pierce, and R. J. Celotta, Rev. Sci. Instrum. **57**, 1314 (1986); M. R. Scheinfein, D. T. Pierce, J. Unguris, J. J. McClelland, R. J. Celotta, and M. H. Kelley, *ibid.* **60**, 1 (1989).
[18] G. Bochi, C. A. Ballentine, H. E. Englefield, S. S. Bogomolov, C. V. Thompson, and R. C. O'Handley, in *Magnetic Ultrathin Films and Surfaces/Interfaces and Characterization*, edited by B. T. Jonker *et al.*, MRS Symposia Proceedings No. 313 (Materials Research Society, Pittsburgh, 1993), p. 309.
[19] R. D. Cowan, *The Theory of Atomic Structure and Spectra* (University of California Press, Berkeley, 1981).
[20] The crystal field is more important in the case of magnetic circular dichroism, which depends strongly on the orbital magnetic moment. See Refs. 21 and 22.
[21] G. van der Laan and B. T. Thole, J. Phys. Condens. Matter **4**, 4181 (1992).
[22] T. Jo and G. A. Sawatzky, Phys. Rev. B **43**, 8771 (1991).
[23] G. Rossi, F. Sirotti, N. A. Cherepkov, F. Combet Farnoux, and G. Panaccione, Solid State Commun. **90**, 557 (1994).
[24] E. Tamura, G. D. Waddill, J. G. Tobin, and P. A. Sterne, Phys. Rev. Lett. **73**, 1533 (1994).
[25] G. van der Laan, J. Phys. Condens. Matter **3**, 7443 (1991).
[26] Ch. Roth, F. U. Hillebrecht, W. G. Park, H. B. Rose, and E. Kisker, Phys. Rev. Lett. **73**, 1963 (1994).
[27] H. Ebert, J. Phys. Condens. Matter **1**, 9111 (1989).